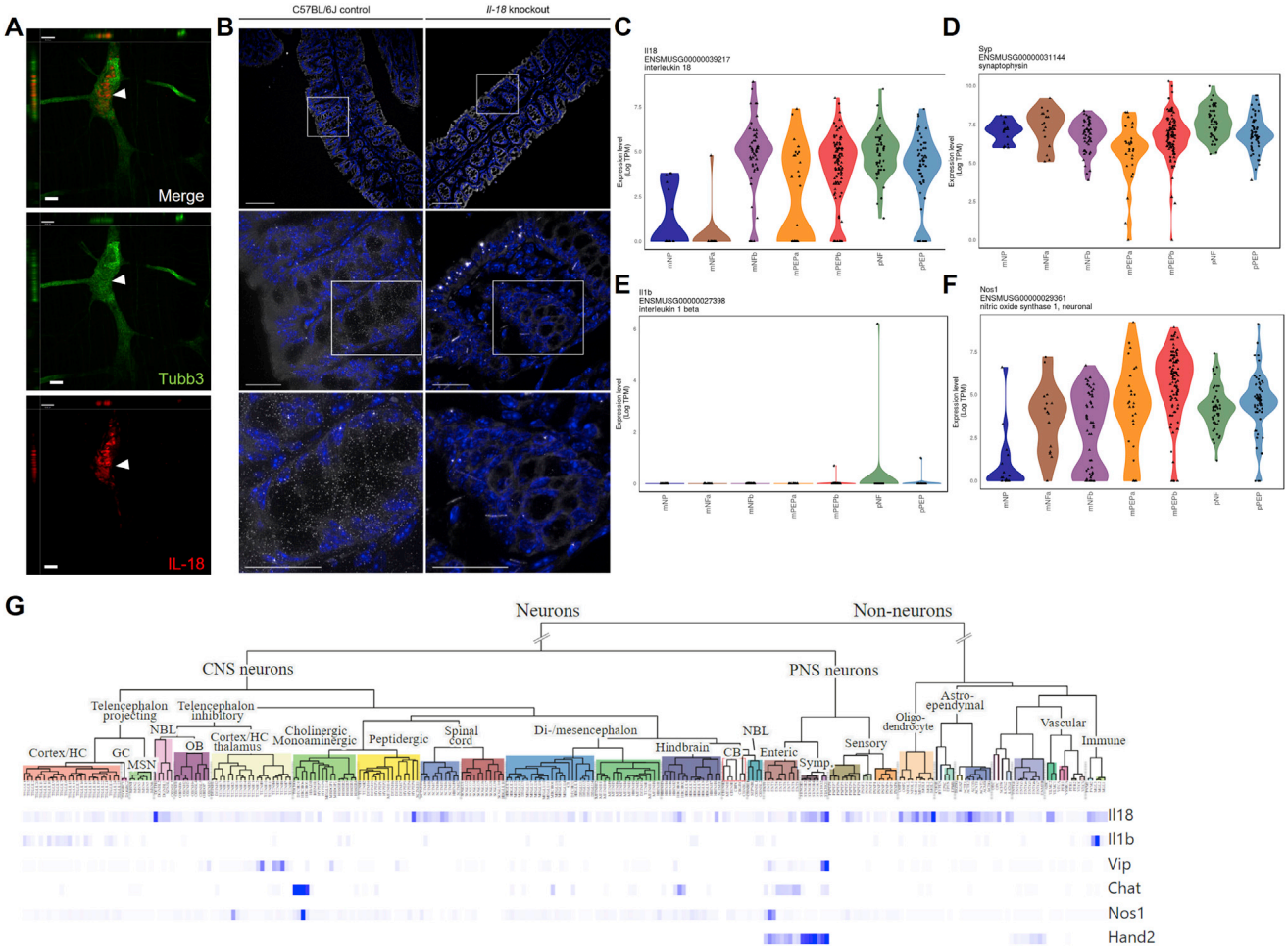

Figure S1. Colonic Neurons Express IL-18, Related to Figure 2

A) Orthogonal view from different planes (x/y, x/z or y/z) of a confocal fluorescence microscopy image used to analyze IL-18+ neurons. IL-18 is red, tubb3 (pan-neuronal marker) is green. Scale bar represents 53 μm. B) Visualization of *Il18* mRNA (white) and DAPI (blue) in wild-type or $Il18^{-/-}$ mouse colon by smFISH. Data show loss of signal of *Il18* mRNA probes in $Il18^{-/-}$ mouse colon. Scale bars represent 25 μm. C-F) Violin plots showing expression and distribution of indicated genes in colonic afferent dorsal root ganglia. Data are from a single-cell RNA-sequencing dataset from Hockley, Taylor et al., 2019 and plots were created using the online database search tool https://hockley.shinyapps.io/ColonicRNAseq/). C) IL-18 has similar expression values as the neuronal marker gene D) synapthophysin. E) Minimal expression of IL-1β is observe in neurons. F) IL-18 is expressed in the same neuron populations that express Nos1. C-F) Neuronal populations abbreviations: mNP (mNonPeptidergic), mNFa (mNeuroFilament-a), mNFb (mNeuroFilament-b), mPEPa (mPeptidergic-a), mPEPb (mPeptidergic-a), pNF (pelvic NeuroFilament) and pPEP (pelvic Peptidergic). TPM (Transcripts Per Kilobase Million). G) Dendrogram showing expression of indicated genes in cell populations generated through analysis of single-cell sequencing of cells in the peripheral nervous system, central nervous system, ENS and immune compartment. Data are from a single-cell RNA-sequencing dataset from Zeisel, Hochgerner et al., 2018 and plots were created using the online database search tool (http://mousebrain.org/genesearch.html).

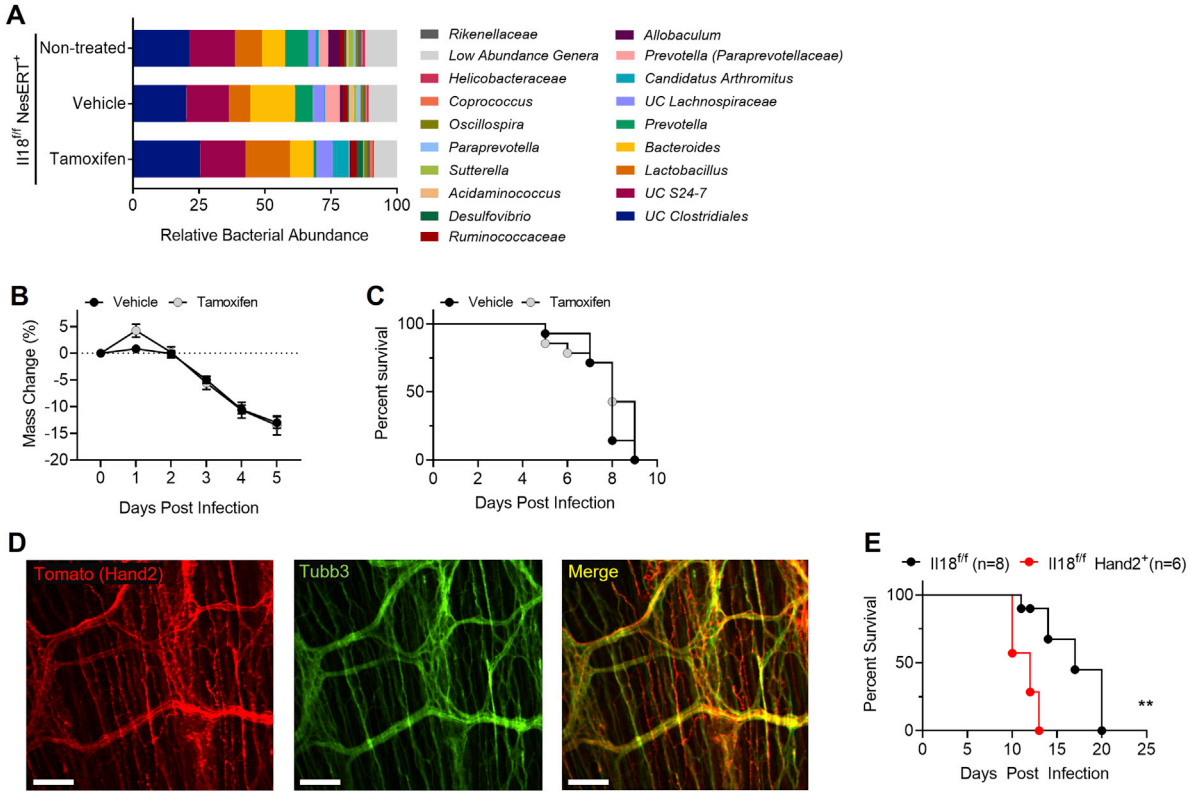

Figure S2. Control Experiments for Tamoxifen, Hand2-Cre and *S.t.* Experiments, Related to Figure 3

A) Average relative abundance of bacterial genera in the fecal intestinal microbiota of $Il18^{f/f}$ $NesERT^{+}$ at steady state and after a regime of 5 daily Tamoxifen or vehicle control injections and a 7 day rest period. Tamoxifen treated mice were housed separate from vehicle mice to inhibit artifacts due to coprophagy. The average relative abundance of bacterial genera in the fecal intestinal microbiota of each group are representative. Values represent 5 $\leq$ pooled averages of mice in the same group. No significant difference in colitogenic or dysbiotic bacteria were discovered by Lefse analysis. B) Weight loss of wild-type C57BL/6J mice pretreated with tamoxifen (n = 14) or vehicle (n = 14) then infected with *S.t.* C) Survival curve for *S.t.*-infected wild-type C57BL/6J mice pretreated with streptomycin and tamoxifen (n = 14) or vehicle (n = 14). D) Whole mount microscopy of the myenteric plexus of $Hand2^{+}Rosa26^{loxStoplox}TdTomoto$ mice demonstrates colocalization of Tomato with the pan-neuronal marker Tubb3. E) Survival curve for *S.t.*-infected $Il18^{f/f}$ (n = 8) or $Il18^{f/f}Hand2^{+}$ (n = 6) mice with no streptomycin pretreatment. Log Rank test was used for analysis. $^{**}p < 0.01$

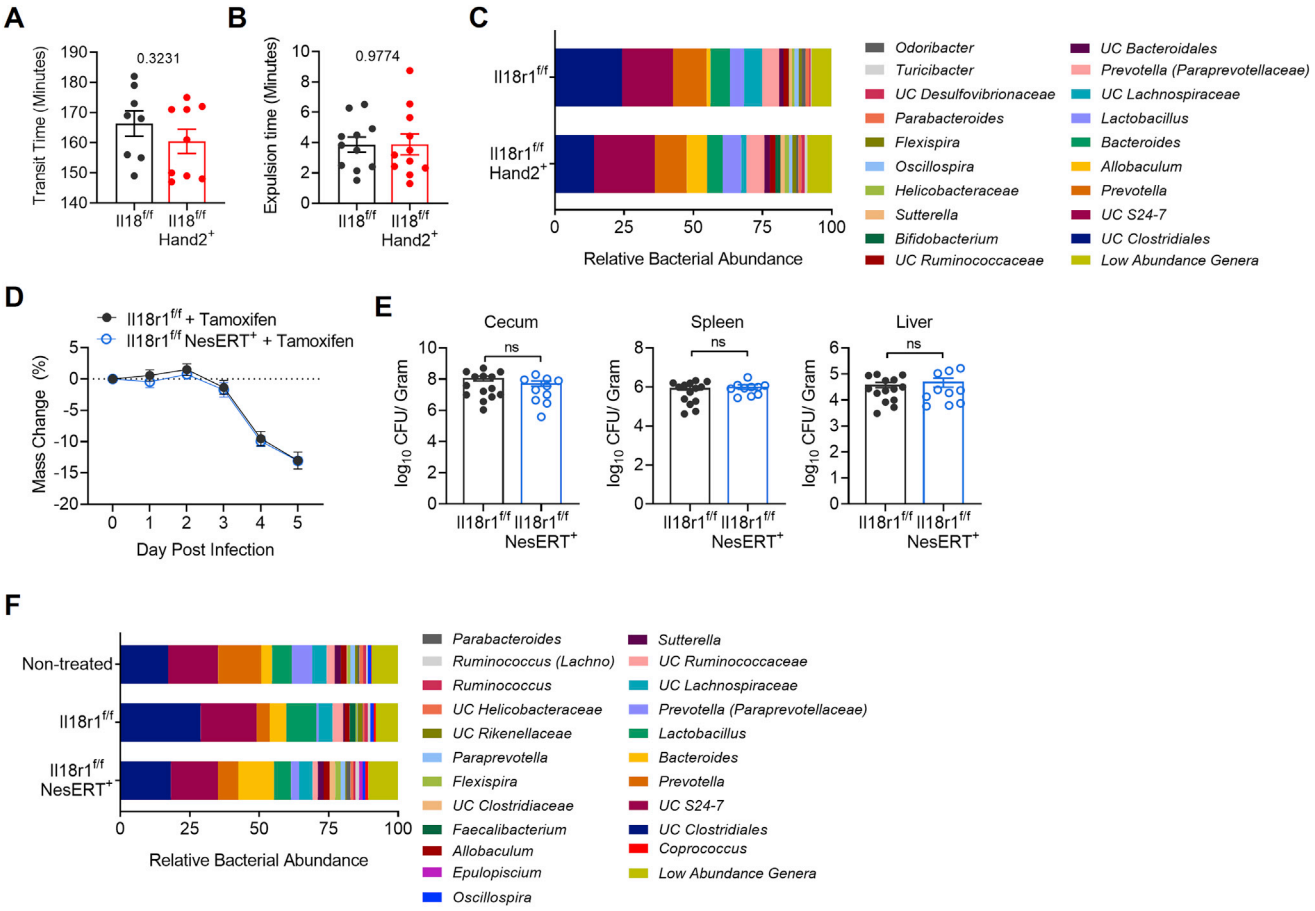

Figure S3. Neuronal IL-18 Does Not Act Intrinsically on Intestinal Neurons to Protect Against *S.t.* Infection, Related to Figure 4.

A) Il18$^{f/f}$ (n = 8) or Il18$^{f/f}$Hand2^{+} (n = 9) mice were gavaged with a red dye (Carmine red) and observed until the dye could be seen in the feces, this time was recorded as the transit time. Each dot represents one mouse and data represent mean ± SEM, unpaired t test was used for statistical analysis. p value is recorded above graph. B) A 3mm glass bead was inserted 2 cm up the colon of Il18$^{f/f}$ (n = 11) or Il18$^{f/f}$Hand2^{+} (n = 11) mice and expulsion time was determined by observation. Each dot represents one mouse and data represent mean ± SEM, unpaired t test was used for statistical analysis. p value is recorded above graph. C) Average relative abundance of bacterial genera in the fecal intestinal microbiota of steady-state littermate cohoused Il18r1$^{f/f}$ and Il18r1$^{f/f}$Hand2^{+} mice. The average relative abundance of bacterial genera in the fecal intestinal microbiota of each group are representative. Values represent pooled averages of 5 ≤ mice in the same group. No significant difference in colitogenic or dysbiotic bacteria were discovered by Lefse analysis. D) Weight loss of Il18r1$^{f/f}$ (n = 14) and Il18r1$^{f/f}$NesERT^{+} (n = 10) mice pretreated with tamoxifen then infected with *S.t.* E) *S.t.* CFU/g of cecum, spleen and liver from Il18r1$^{f/f}$ (n = 14) and Il18r1$^{f/f}$NesERT^{+} (n = 10) mice pretreated with tamoxifen 5 days post infection. Each dot represents one mouse. Data represent mean ± SEM, Mann-Whitney test was used for statistical analysis. ns: not significant, p > 0.05. F) Average relative abundance of bacterial genera in the fecal intestinal microbiota of Il18r1$^{f/f}$ and Il18r1$^{f/f}$NesERT^{+} after 5 day treatment with tamoxifen and a 7 day rest period. Non-treated animals are Il18r1$^{f/f}$. The average relative abundance of bacterial genera in the fecal intestinal microbiota of each group are representative. Values represent pooled averages of 5 ≤ mice in the same group. No significant difference in colitogenic or dysbiotic bacteria were discovered by Lefse analysis.

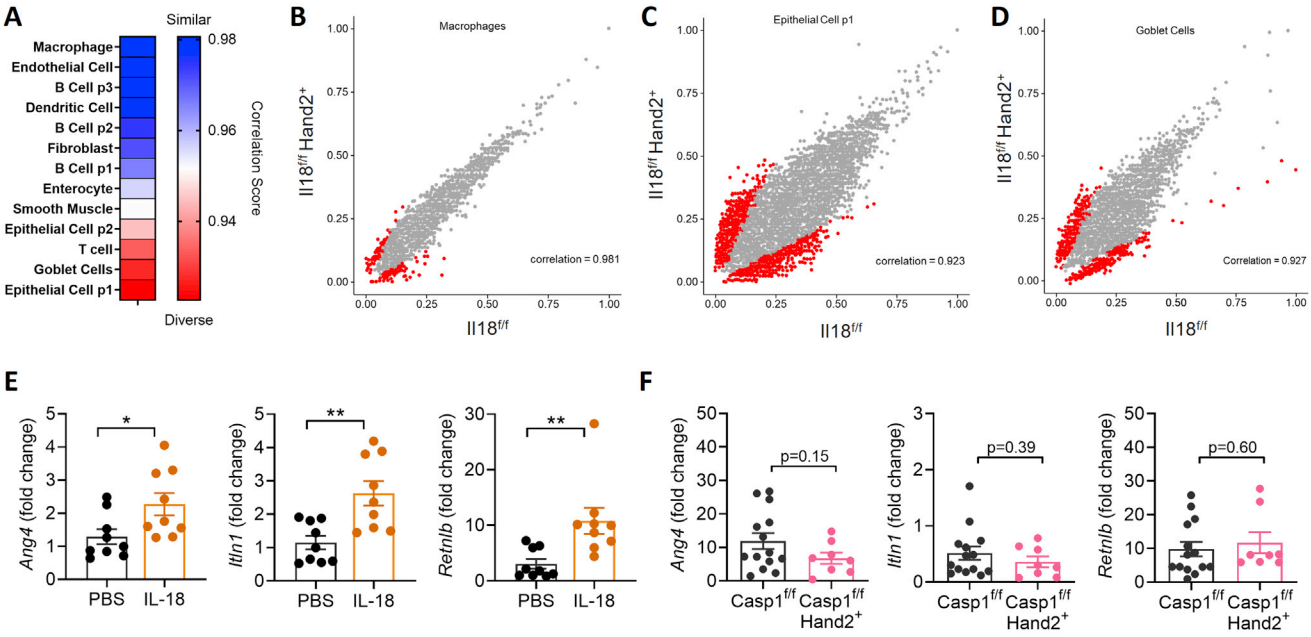

Figure S4. Correlation Analysis of Clusters between Il18$^{f/f}$ and Il18$^{f/f}$ Hand2^{+} Mice Identifies that Neuron-Derived IL-18 Drives AMP Production by Goblet Cells Independent of Caspase 1, Related to Figure 5

A) Correlation analysis of each cell cluster from Il18$^{f/f}$ and Il18$^{f/f}$Hand2^{+}. Higher correlation value (depicted in blue) indicates the gene expression pattern in that cluster is similar between Il18$^{f/f}$ and Il18$^{f/f}$Hand2^{+} samples. Lower correlation value (depicted in red) indicates the gene expression pattern in that cluster is dissimilar between Il18$^{f/f}$ and Il18$^{f/f}$Hand2^{+} samples. B-D) Scatterplot analysis comparing average gene expression of genes in B) macrophages, C) epithelial cell p1 and D) goblet cells between Il18$^{f/f}$ and Il18$^{f/f}$Hand2^{+} groups. Significantly differentially regulated genes (Log_2FoldChange ±) are depicted in red. E,F) Expression of the AMPs *Ang4*, *Itln1*, and *Retnlb* in tissue biopsies from the proximal colon of E) Il18$^{f/f}$Hand2^{+} mice treated for 5 days with 1 ug/ mouse of rIL-18 or PBS by intraperitoneal injection or F) Il18$^{f/f}$ and Il18$^{f/f}$Casp1^{+} mice. Each dot represents one mouse, and data represent mean ± SEM. Unpaired t test was used for statistical analysis. *p < 0.05, **p < 0.01.

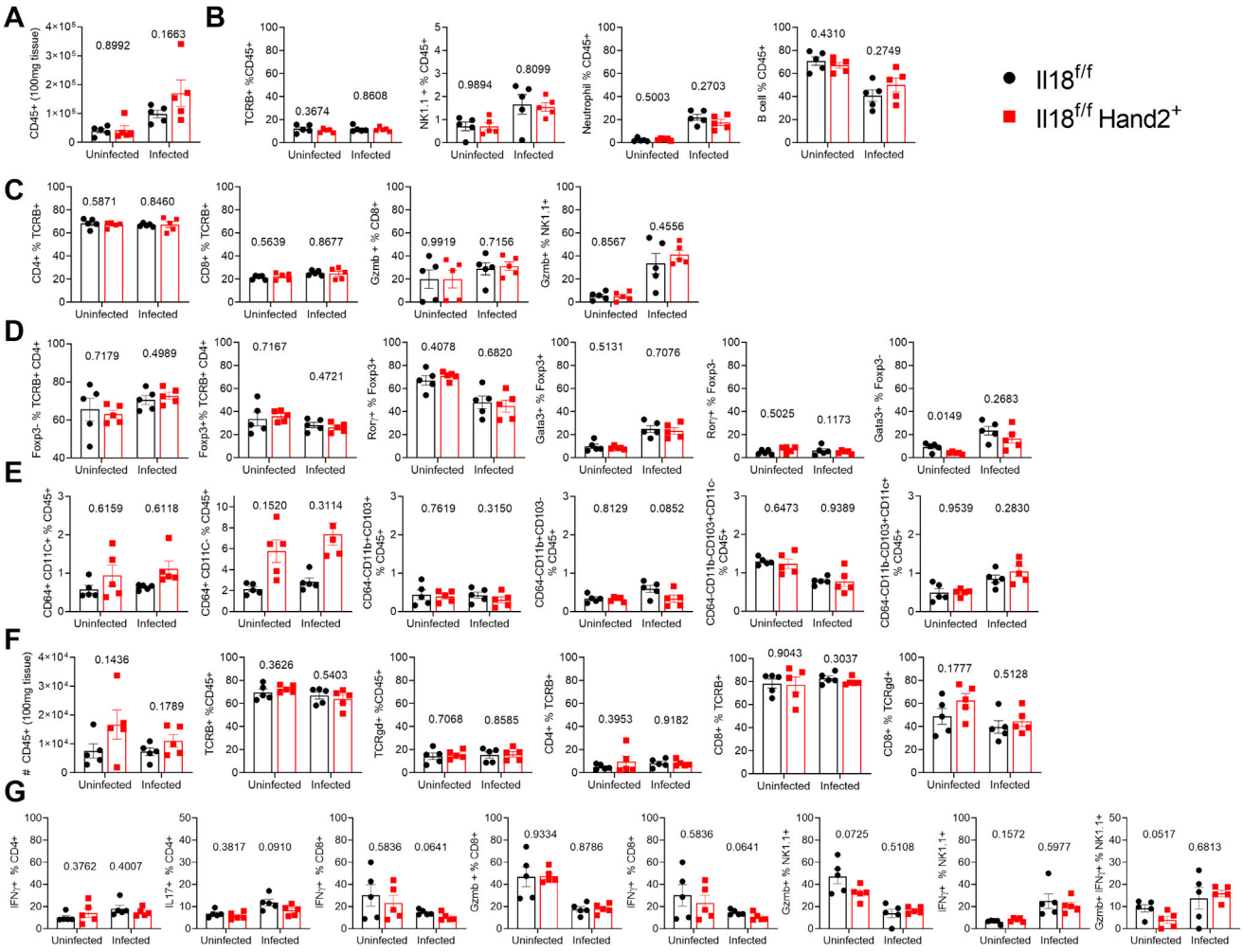

Figure S5. Neuronal IL-18 Does Not Alter the Colonic Immune Cell Compartment at Steady State or during *S*.t Infection, Related to Figure 6

Flow cytometry analysis of steady state Il18$^{f/f}$ and Il18$^{f/f}$Hand2^{+} colons or Il18$^{f/f}$ and Il18$^{f/f}$Hand2^{+} colons 48 h post infection with *S*. typhimurium. A-E) Cell number or % of parent population for immune cell subsets from the lamina propria and muscularis layer of the colon. A) Number of live CD45+ cells in 100mg of total colon tissue. B) % of live CD45+ cells. TCRB+ (B220- CD19- CD326- CD11b- IA/IE- NK1.1- TCRB+ CD45+). Nk1.1+ (B220-CD19- CD326- CD11b- IA/IE- CD4- CD8- TCRB- NK1.1+ CD45+). B cell (CD326- TCRB- CD3- B220+ CD19+ CD45+). Neutrophil (CD326- TCRB- CD3- CD19- Ly6g+ CD45+). C) % parent population. TCRB+ (Dump-(B220- CD19- CD326- CD11b- IA/IE-) TCRB+ CD45+). CD4+ (Dump- CD8- CD4+ TCRB+ CD45+). CD8+ (Dump- CD4- CD8+ TCRB+ CD45+). Nk1.1+ (Dump- CD8- Cd4- TCRB- Nk1.1+ CD45+). D) % of parent population. TCRB+ CD4+ (Dump- (CD326- CD8- CD19- B220- IA/IE-) CD4+ TCRB+ CD45+). Foxp3+ (Dump- CD4+ TCRB+ Foxp3+ CD45+). Foxp3- (Dump- CD4+ TCRB+ Foxp3- CD45+). E) % of live CD45+ cells. CD64+ CD11C+ (Dump- (CD326- TCRB- CD3- CD19- CD90.2-) CD64+ CD11C+ IA/IE+ CD45+). CD64- CD11b+ CD103+ (Dump- CD64- CD11b+ CD103+ CD45+). CD64- CD11b+ CD103- (Dump- CD64- CD11b+ CD103- CD45+). CD64- CD11b- CD103+ CD11c- (Dump- CD64- CD11b- CD103+ CD11c- CD45+). CD64- CD11b- CD103+ CD11c+ (Dump- CD64- CD11b- CD103+ CD11c+ CD45+). F) Cell number or % of parent population for immune cell subsets in the intraepithelial layer. CD45+ (Live CD45+ cells). TCRB+ (CD326- Nk1.1- TCRGD- TCRB+ CD45+). TCRGD+ (CD326- NK1.1- TCRGD+ TCRB- CD45+). G) Isolated single cells from the colon were stimulated *in vitro* with PMA and ionomycin for four h, with the addition of Brefeldin A 1 h into the stimulation. Cells were then processed for intracellular cytokine analysis. CD4+ (Dump- (CD19- CD11B- B220-) CD8- CD4+ CD45+). CD8+ (Dump- CD4- CD8+ CD45+). Nk1.1+ (Dump- CD4- CD8- NK1.1+ CD45+). (A-G) Each dot represents one mouse and data represent mean ± SEM. Unpaired t test was used for statistical analysis and p value is annotated.

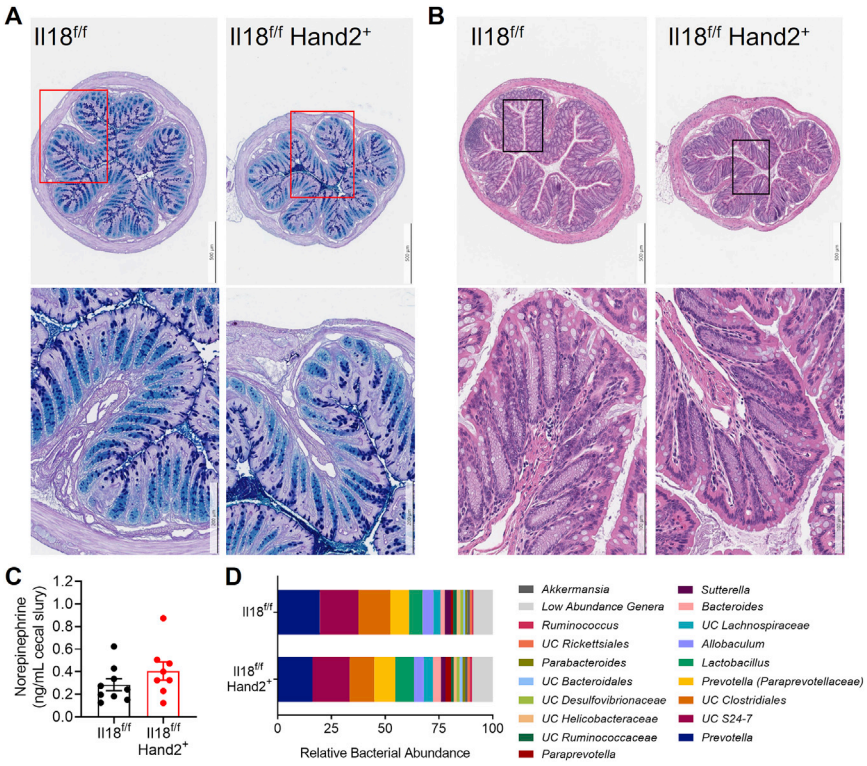

Figure S6. Neuronal IL-18 Does Not Affect Luminal Catecholamines, Bacterial Relative Abundance, Goblet Cell Development, or Gross Intestinal Architecture, Related to Figure 6

A) AB/Pas staining or B) H&E staining of colon cross-sections from $Il18^{f/f}$ and $Il18^{f/f}Hand2^{+}$ mice. Data are representative of tissue sections from three mice of each genotype. C) Noradrenaline levels in the cecal contents of $Il18^{f/f}$ and $Il18^{f/f}Hand2^{+}$ mice. Each dot represents one mouse and data are representative of mean ± SEM. Unpaired t test was used for statistical analysis. D) Average relative abundance of bacterial genera in the fecal intestinal microbiota of steady-state littermate cohoused $Il18^{f/f}$ and $Il18^{f/f}Hand2^{+}$ mice. The average relative abundance of bacterial genera in the fecal intestinal microbiota of each group are representative. Values represent pooled averages of 5 $\leq$ mice in the same group. No significant difference in colitogenic or dysbiotic bacteria were discovered by Lefse analysis.